GEOLOGICAL INVESTIGATIONS

Z-MORH TUNNEL PROJECT

SRINAGAR, (J & K)

Introduction:

Ladakh area of Jammu and Kashmir is linked with rest of the country through two routes Leh - Srinagar and Leh – Manali which remain closed in the months of November to March every year due to heavy snow fall. To overcome this isolation of Ladakh region, Boarder Roads Organization has planned two tunnels in the difficult areas of the National Highway 1D.

Proposed Z-Morh tunnel site is located 2.7 km from Sonamarg towards Srinagar near the village Sitkhari. The Eastern portal of the Z-Morh tunnel is located about 400mt from the Shitkari bridge of Sonamarg Town on the Srinagar side, whereas the western portal of the tunnel is planned at the village Gagangir towards the Sonamarg (Fig. 1). The tunnel is aligned nearly in the east west direction.

Geological mapping has been done on 1: 1000 scale during the topographic survey of the area itself. The geological map in this report is being produced on much reduced scale. A number of sections have been developed across the tunnel alignment as well as along the tentative tunnel alignment.

Contribution to these studies has been made by Dr. G.C.S.Gaur and Mr. Ravi Negi of M/S G S GeoEnVirons Pvt. Ltd. and Dr. Mahendra Singh of Civil Engineering Department, IIT Roorkee.

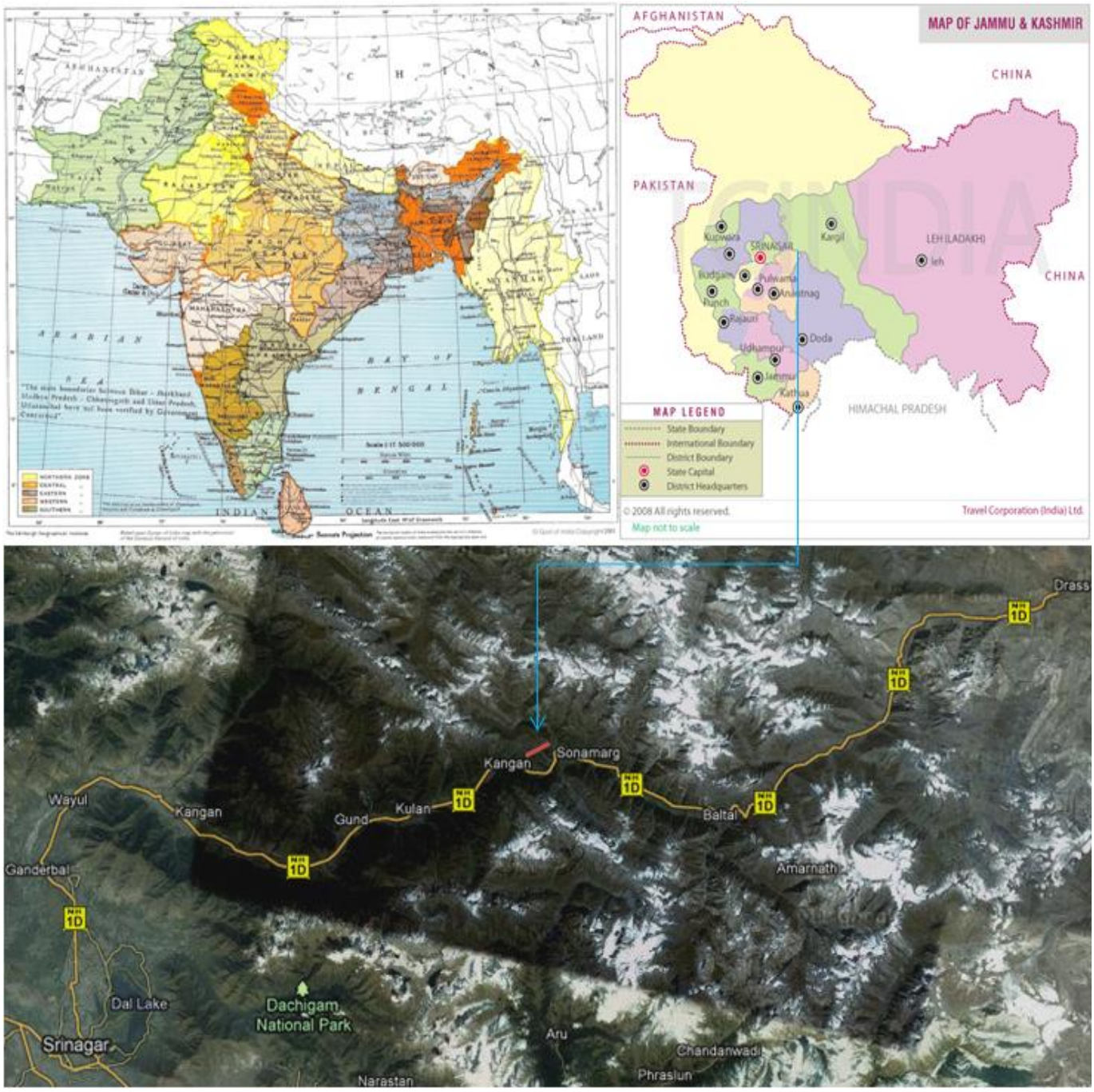

Fig. 1. Location map of the project area

Geomorphology

The area exhibits an undulating and rugged topography with highly mountainous terrain having little vegetation. The mountains are composed of sedimentary and igneous rocks which are being subjected to severe cold weathering. The altitude varies between 2500-3800 m above MSL. Hill faces are made up of high rocky escarpments (Fig. 2), steep slopes and moderate – Gentle slopes made up of slided debris. Cliffs are high and barren. On both the portals of proposed Tunnel slided debris is found. Sonamarg as well as Gangangir towns are located on the slided debris (Fig.3).

Most of the settlements on the lower elevations are also located on slided debris. On both the flanks of the river Sindh the ridges are oriented in NE-SW direction.

Area is drained by the mighty turbulent river Sindh. Sindh is the largest river of the valley of Kashmir. It flows through wide valley having gentle gradient (Fig. 4), whereas its tributaries are always steep and U shaped. Drainage in the area is parallel to sub-parallel and sub dendritic. Its tributary Shitkari nala passes by the side of eastern portal and along western portal Shutiyan nala passes both the nalas join the river sindh nearly at right angle.

Fig. 2 A view of high cliff and Escarpments.

Fig.3 A view of Sonamarg Town

Fig 4 A view of Sindh River near Eastern Portal, Z-Morh

Regional Geology:

The earliest reference to the geology of Ladakh region is available from the works of Thompson (1852), Stoliczka (1866), Drew (1875), and Lydekker (1880-83). The latter studied the western part of the Ladakh along Sonamarg-Zozi la-Dras belt and followed the classification based on Palaeo-Mesozoic succession of Kashmir (Middlemiss, 1910).

The comprehensive studies including mapping were undertaken by Wadia (1937), in Gilgit and Astor region. In continuation, the work on this belt was carried out by Kohli, Sahni and Bhatnagar (1958).

The Tethyan rocks of Kashmir which override the Indus belt consist chiefly of Triassic-Jurassic sediments, though in the basement high zone of the Nun-Kun axis which extends along the Suru Valley, older rocks override the belt.

Regional geological / lithostratigraphical map of the area is given in the Fig.5 and the Lithostratigraphy of the region is described in the table 01.

Table 01 Lithostratigraphic Succession of the area around Z-Morh.

Facies	**Formation**	**Members**
Indus Flych Sediments	Kargil Formation	
	~~~~ Kargil Thrust or Unconformity ~~~~	
Indus facies	Dras Formation	Maman Phyllite Serpentine- Chromitite- Dunite Radiolarian chert, Limestone and mélange

		Lava and agglomerates Changthang slate
	~~~~~~~~ Dras Thrust ~~~~~~~~	
Tethyan facies	Matayin Limestone Zozi la Formation Panzal trap Agglomerate slate Tertiary Granite (Intrusive in Indus facies)	
	~~ Kargil Thrust or Unconformity ~~	
Granite Group	Ladakh Granite (Northern basement)	

Agglomerate slate:

Fine grained gray to black colored sedimentary rock formation is known as Agglomerate slate. Formation is exposed in the core of the Zozi- La anticline between Gumri nallah and Machoi nallah. This formation consists of dark colored slates and grey colored Phyillites with alternating bands of Pyrite greywacke.

This assemblage lithologically resembles with the Agglomeratic slates from rest of Kashmir. The Agglomerate slates are the oldest exposed unit in the Zozi –La anticline,

This formation is underlain by the Panjal trap.

Panjal trap:

The Agglomeratic slate is overlain by a band of green partly schistose basic lava, which is considerably metamorphosed giving resemblance of green schist. The volcanic textures and structures such as the pillows are often faithfully preserved at a number of places, especially near Minamarg.

A small patch of Panjal trap is also exposed near Zoji- La within another small anticline and is visible on the cliff to the east of the Pass.

Zoji- La Formation:

A large severely folded belt comprising of grey and brown Phyllites with bands of limestone's and pyritic shale, is found exposed immediately overlying the Panjal trap in the area and is in turn overlain by the thick massive Matayain Limestone.

On the basis of Fragments of fossil Ptychites found at Thajwas, it has been referred as Muschelkalk by many workers. This formation has been given the name "Serzing phyllite" by Raiverman and Mishra (op.cit) in the eastern part, but they have made no reference to the western outcrop in Zoji-la and Thajwas.

Matayin Limestone:

Throughout the southern part of the area a thick zone of limestone, partly dolomite, is found exposed from Sonamarg to southeast of Dras and from Gyal through south of Mulbekh. In the Sonamarg- Baltal section this limestone is exposed in a syncline flanked by the Zoji-La formation of Thajwas and Zoji-La on either side. In Matayin, it overlies conformably the Zoji-La formation and in the east it has been partly cut off by Dras thrust.

In the Zoji-La section, the upper part of Zoji-La formation consist of black shale which passes gradually upwards in to thin bedded platy limestone having frequent marly bands and topped by a considerable thickness of massive dolomite.

Dras Formation

Dras formation is over 3,000m thick and consists of a complex of sedimentary and igneous suite of rocks. The basal unit of the formation exposed in the east near Changthang and persisting through Shergol to

Namikala, consist mostly of dark grey slates, slaty shale and occasional limestone, with which bands of greywacke and purple radiolarian chert are interbedded.

The middle unit consists of enormous thickness of basic lava, agglomerate, tuff, ash beds and numerous bands of lensoid jasparite, chert, calcilutite and shale.
The upper part of the Dras formation comprises a thick suite of severely controlled calcareous phyllite with interbedded chert and greywacke. It lies in immediate contact with the Dras Thrust.

Kargil Formation

In the Kargil area the formation rests unconformably on the Ladakh Granite and has a gentle southerly dip, the contact being marked by a zone of conglomerate containing boulders of granite and rocks of Dras Formation. This is succeeded by a thick sequence of sandstone and shale containing fresh water mollusks. The southern limit of Kargil belt is bound by a thrust, the Kargil Thrust, along which the Dras Formation comes in juxtaposition with these rocks. The upper part is thus truncated by a thrust and accordingly the complete thickness of the formation is not exposed.
The belt continues eastwards within the same tectonic setting as far as Hagins-Shakardeo. A noteworthy feature is that there is a continuous lateral and vertical variation of facies, with the addition of new lithological elements towards the base. The conglomerate-sandstone sequence in Hagins is not the basal unit but lies towards the middle whereas the base consists of a sequence of dark-grey shale-greywacke rhythmites. This zone becomes very thick to the east in Khalsi and beyond, where almost a complete sequence of greywacke, shale and limestone rhythm is exposed. This facies of rocks has usually been referred to as “Indus Flysch” while the Kargil sequence as “Ladakh Molasse”.

It is interesting to note that the “flysch” facies in the eastern part is a marine one as is evidenced from the presence of marine foraminifera, suggesting an early to the late Cretaceous age, (Pande *et.* al., 1969), whereas the “molasse” of Kargil indicates a fresh water facies as indicated by its fauna and it is essentially Tertiary in age. This is a case of lateral and vertical variation of facies wherein the Cretaceous “flysch” sequence passes outwards to southwest and upwards into Tertiary “Molasse” sequence. Equivalents of Kargil Formation are also exposed to south of the main belt resting directly on the folded Dras Formation. These rocks occur as outliers, like the outcrops of Cheskor and

Batambas, or are caught up within the imbricate structures of the Dras Formation towards the southern part of the Dras belt.

Geology of the area

Geological mapping has been carried out on 1:1000 scale (Fig. 6). Detailed structural data has been collected and plotted on the same scale (Fig. 7). A series of geological section have been developed based on surface data for geological interpretation (Fig. 8-15).

Lithostratigraphy in the area can be described as follows:

RECENT	River born material
	Debris and Talus material
PERMO- CARBONIFEROUS	Zoji-La formation
	Panjal Trap

RIVER BORN MATERIAL:

River Born Material is found deposited in the river bed. It consists of loose large boulders, pebbles, grit, sand and silt. This material is continuously modified during the floods.

DEBRIS AND TALUS MATERIAL:

Thick amount of Talus /Debris materials are found all along the base of the ridge. Debris materials are product of physical weathering at the top of the ridge from where it flows downwards. Debris material consists of large coarse angular fragments. These rock fragments are often found embedded in the loose matrix of grit, sand silt and clay. This has attained stability in due course of time

At places slided debris mass is found forming large grounds, such as Sonamarg town area (Fig 3). The slided debris is also found along the river banks and receding path of glaciers (Fig. 16).

Fig 16 large amount of Debris material is found along the river Sind

ZOJI-LA FORMATION

Large severely folded units consisting of dark grey graphitic phyllites are found in the eastern part of the project. These phyllites are finely foliated in which fine platy minerals impart shining texture to the rocks (fig.17). along the foliation planes extremely fine grained lenticular silica veins are observed. At places with in these phyllites fine pyrite cubes are noted in abundance. (fig.18)

Slaty cleavage is also noted at certain places with in these phyllites. In the area, these phyllites have steep dip of foliation. Rocks are also jointed, but these joints do not persist for long.

Zoji-La formation is found in the area of proposed Eastern portal site. Rock formation is phyllitic slate in nature. These slaty rocks consist of fine grained calcareous and basic mineral assemblage. Fine grained high cleaved, fragile dark brown to black colour slates are phyllitic in nature. Pyrites cubes of varying size from 1mm to 7mm are often found in these rocks. these slates grade upward into dark grey slates and calcilutite with occasional fine bands of calcarenite (fig.19).

Fig. 17 View of dark grey slates of Zoji-La Formation

Fig.18 A Close View of Zoji-la slate having Pyrite cubes

Fig.19 A Close view of highly cleaved dark –Grey slates of Zoji-La Fromation

PANJAL TRAP

Dark green colored basic rocks belonging to Panjal trap are found in the proposed project site area. Often these metabasics, due to leaching give brown colored look. Hard, compact, massive 1-20 m thick different types of trap are being observed in the proposed project area. These Meta basics range from massive to schistose character in nature.

Panjal Trap formation consists of basic minerals like Amphiboles, Hornblende, Plagioclase and Olivine. The Panjal Traps are made up of Plagioclase-Pyroxene assemblage. Amphiboles and Plagioclase mineral assemblage dominates throughout the whole lava flow sequence. These rocks are dominantly basaltic-andesitic and show a compositional and environmental affinity with accreting plate margin lava. Rocks are mostly fresh, but often shallow weathering is noted at certain places. Leaching of iron minerals is also profound in the area, which imparts brown color to the rock on the surface.

The Panjal Trap is a greenish to brownish color rock with some dark grey varieties. They are very hard, compact; massive, and generally fine-grained. Compact mass of fine grained material often shows amygdaloidal structure (Fig.20). Chlorite, quartz and epidote fillings are found in the cavities. Vesicular structure is also found in these traps. The vesicles, range in size from small speck to more than 5 cm (longest-axis) (Fig 21). Most of the vesicles are elongated in shape. Rounded vesicles are common in the project area. Quartz veins are commonly found traversing these rocks along bedding planes, joints and fractures (Fig. 22).The Panjal Trap is semi crystalline aggregate of Plagioclase, Amphiboles and Pyroxene with a mesostasis in which microlites of these minerals and their alteration products are found embedded in the devitrified glass in the groundmass. Opaque minerals, varying in size from fine microscopic dust to small micro -phenocrysts, are common throughout the whole sequence of lava beds. Coarse grained hornblende crystals provide porphyritic texture to the rocks (Fig. 23). Large pyrite crystals are also found in these rocks (Fig. 24). Along joints and foliations often serpentine minerals are also found as veins (Fig. 25).

In the microscopic observations Plagioclase minerals occur in three sizes—mega-phenocrysts, micro-phenocrysts, and minute microlites. Mega-phenocrysts, sometimes altered to kaolin, are confined to the lower two flows whereas the micro-phenocryst and microlites form a common feature of the whole lava sequence. The mega-phenocrysts, in general, and some micro-phenocrysts are fractured in which these fractures are often healed up with green chlorite and epidote. The phenocrysts may have been

subjected to stress during the upward movement of the magma at the time of eruption causing fractures in the entertained crystals. The composition of the plagioclase is variable and has a close correlation with the size of this mineral. The magaphenocrysts, found only in the lower two flows, are highly calcic; their compositional range is between Bytownite and labrodorite (An_{82}-An_{56}). The composition changes from calcic to sodic plagioclase with the decrease in size of the phenocrysts. Zoning towards decreasing An-content is observed along the peripheral portion of some crystals. Hornblende, peridote, pyroxene, olivine are other dominating minerals in the assemblage. Pyrite cubes are found in the ground mass as minor mineral.

Fig. 20 A View of amygdaloidal basic rock

Fig. 21 A View of Vesicular basic rock

Fig. 22 Silica veins are common in the rock formation

Fig. 23 Coarse Hornblende crystals form Porphyritic texture in the rock

Fig. 24 Pyrite cubes are often found in these rocks.

Fig. 25 Serpentine veins are also found along the joints & foliations in the basic rock

STUCTURE OF THE AREA

Rocks are found all over the project area excepts few regions where rocks are covered with debris and soil deposits. All structural data have been plotted and shown in the structural map (fig 6). Major structural features especially discontinuities are: Foliation, Joints, Shear planes and Shear zones.

Foliation:

Foliation planes are marked by sheet differentiations in the rocks. Orientation and colour of minerals also define the foliation planes (Fig. 26). Rocks are having Steep dip in the entire area. In the massive rocks foliation planes are nearly 1m to 1.5m apart, whereas in the schistose rocks these foliations are closely packed. The foliation varies as follows:

Location	Strike	Dip	Direction
Near the bend (East portal)	$N153^0$ – $N 333^0$	37^0	$N 243^0$
Eastern Portal near drilling area	$N 122^0$ - $N 302^0$	43^0	$N 212^0$
Near Toll barrier area	$N 120^0$ - $N 300^0$	73^0	$N 210^0$

Right side of nala (West portal)	N 86^0 – N 176^0	42^0	N 356^0
Left side of nala (west portal)	N 105^0 – N 195^0	47^0	N 15^0

Fig 26 Thin layers of foliated Meta basic rocks near the western portal area.

Joints:

Rocks are highly jointed and fractured three to four sets of joints are most predominant in the area. All the major joints persist for quite long distance (Fig. 27 to 30). Often shallow weathering is also noted along these joints. Orientation of these joints have been plotted on stereo net and being given in Fig (31 to 35).

The prominent major joint sets are as follows:

Prominent Joint sets near the Bridge area

Sets No.	Strike	Dip	Directions	Remarks	Description of Discontinuities
1	$N60^0$- $N 240^0$	34^0	$N 330^0$	Open joint set with the gap of 0.5- 1 cm, filled with clay and weathered materials. Persist for 10 to 12m. 2 to 3 m apart.	Rough (Planar)
2	$N 30^0$- $N 210^0$	85^0	$N 300^0$	Open joint with the gap of 1-2cm filled with clay and weathered materials Persist for 5 to 7m. 1 to 3 m apart.	Rough (Planar)
3	$N 25^0$- $N 205^0$	45^0	$N 295^0$	Open joint with the gap of 1 cm filled with clay and weathered material. Persist for 5 to 6m. 3 to 5 m apart.	Rough (Planar)
4	$N 108^0$- $N 288^0$	76^0	$N 198^0$	Open joint with the gap of 5-7 cm filled with clay and weathered material. Persist for 35 to 40m. 2 to5m apart.	Rough (Undulating)
5	$N 32^0$- $N 212^0$	61^0	$N 302^0$	Closed set of joint, persist for 30-35m.	Rough (Undulating)

Prominent Joint sets near the Drilling area (East Portal)

Sets No.	Strike	Dip	Directions	Remarks	Description of Discontinuities
1	N81°-261°	23^0	N 351°	Open joint with the gap of 1 cm filled with clay and weathered material, persist for 2-3 m.	Slickenside (P lanar)

2	N102°- N 282°	67^0	N 192°	Open joint with the gap of 1-3 cm filled with clay and weathered materials. Persist for 20-22m. 3 to 5 m apart.	Slickenside (Undulating)
3	N 157°- N337°	49^0	N 247°	Open joint with the gap of 1-2cm filled with clay and weathered materials. Persist for 18-20m. 3 to 4m apart.	Rough (Undulating)
4	N52°- N232°	33°	N142°	Open joint with the gap of 1 cm filled with clay and weathered material. Persist for20-22m. 3 to 5 m apart.	Rough (Undulating)
5	N33°-213°	51°	N303°	Open joint with the gap of 0.5-1 cm filled with clay and weathered material. Persist for 20-22m. 1 to 3 m apart.	Rough (Planar)

Prominent Joint sets West portal near right side Nala

Sets No.	Strike	Dip	Directions	Remarks	Description of Discontinuities
1	N 51^0-N231^0	57°	N 321°	Open joint with the gap of 1 cm filled with clay and weathered material. Persist for 1.5-2.0m.	Rough (Undulating)
2	N 39^0-N219°	47^0	N 309^0	Open joint with the gap of 1 cm filled with clay and weathered material. Persist for 1.5-2m.	Rough (Planar)
3	N 45^0- N225^0	59^0	N 315^0	Open joint with the gap of 1 cm filled with clay and weathered material. Persist for 1.0 to 2.0m.	Rough (Planar)

4	N 71^0- N351^0	27^0	N 261^0	Open joint with the gap of 1 cm filled with clay and weathered material. Persist for 2.0 to 2.5m.	Rough (Undulating)
5	N 159^0-339 N^0	12^0	N 249^0	Open joint with the gap of 1 cm filled with clay and weathered material. Persist for 1 to 1.5m.	Smooth (Planar)
6	N71^0-N251°	41^0	N 161^0	Open joint with the gap of 1 cm filled with clay and weathered material. Persist for 2.5 to 3.0m.	Rough (Undulating)
7	N45°-225°	43°	N135°	Open joint with the gap of 1 cm filled with clay and weathered material. Persist for 1 to 1.5m.	Smooth (Planar)
8	N55-°235°	51°	N145°	Open joint with the gap of 1 cm filled with clay and weathered material. Persist for 2 to 2.5m.	Rough (Undulating)

Prominent Joint sets West portal at the left side nala

Sets No.	**Strike**	**Dip**	**Directions**	**Remarks**	**Description of Discontinuities**
1	N 80^0-N260^0	33^0	N 350°	Open joint with the gap of 1-3 cm filled with clay and weathered material. Persist for 1.5 to 2.0m.	Rough (Stepped)
2	N 99^0- N279^0	67^0	N 189^0	Open joint with the gap of 1-2 cm filled with clay and weathered material. Persist for 2.5 to 3m.	Smooth (Planar)
3	N 67^0- N247^0	49^0	N 337^0	Open joint with the gap of 1-2 cm filled with clay and siliceous material. Persist for 1 to 2m.	Rough (Planar)
4	N35^0- N215^0	31^0	N 305^0	Closed set of joint. Persist for 1.5 to	Rough (Undulating)

				2.0 feet.	
5	$N115^0$-$N 295^0$	39^0	$N 205^0$	Open set of joint. Persist for 1 to 2 feet.	Rough (Undulating)
6	N31°-N211°	69°	N301°	Open set of joint. Persist for 1.5 to 2.0m.	Rough (Undulating)

Prominent Joint sets East portal near nala

Sets No.	Strike	Dip	Directions	Remarks	Description of Discontinuities
1	$N 50^0$- $N 230^0$	27^0	$N 320^0$	Open joint with the gap of 0.5-5cm filled with clay and weathered material and Siliceous veins. Persist for 50 to 55m. 4 to 6m apart.	Rough (Planar)
2	$N153^0$- $N333^0$	63^0	$N 243^0$	Closed set of joint Persist for 30-35m. 4 to 5m apart.	Rough (Undulating)
3	$N 71^0$-$N 251^0$	33^0	$N 341^0$	Open joint with the gap of 1 cm filled with clay and weathered material, Persist for20-22m. 3 to 4m apart.	Rough (Undulating)
4	$N 71^0$-$N251^0$	47^0	$N 161^0$	Open joint with the gap of 1 cm filled with clay and weathered material. Persist for 20-22m. 4 to 5m apart.	Slickenside (Undulating)

Prominent Joint sets 400 mt from East portal location

Sets No.	Strike	Dip	Directions	Remarks	Description of Discontinuities
1	N 153^0-N333^0	27^0	N 243^0	Open joint with the gap of 0.5-5 cm filled with clay and weathered material and Siliceous veins.	Rough (Planar)
2	N71^0- N251^0	63^0	N 161^0	Closed set of joint Persist for 3-3.5m.	Rough (Undulating)
3	N 33^0-N 213^0	33^0	N 303^0	Open joint with the gap of 0.5 -1 cm filled with clay and weathered material, Persist for1-1-5 feet.	Rough (Undulating)
4	N 59^0-N239^0	47^0	N 329^0	Open joint with the gap of 1-2 cm filled with weathered material. Persist for 1-2 feet.	Slickenside (Undulating)
5	N167^0-N 347^0	31^0	N 257^0	Open joint with the gap of 1 cm filled with clay and weathered material, Persist for3-4 feet.	Rough (Undulating)
6	N 115^0-N295^0	52^0	N 205^0	Closed joint, Persist for 2-2.5 feet.	Slickenside (Undulating)

Fig. 27 A View of Joint along tunnel alignment, Joints run for more than 30 m.

Fig. 28 A View of joint sets near West portal area

Fig.29 A view of open joints set

Fig.30 A View of Open joints set

Shear planes:

Shearing is often found along few prominent joint (Fig. 36). Along these shear planes, up to 10 cm thick crusted material is observed. Often along these shear planes, open narrow cavities are noted due to the removal of crusted (Soft) material. Most prominent orientation of these shear planes is N 10^0 to N 20^0 at times fine displacement of 5 to 10cm is observed along these shear planes.

Fig 36 A View of Shear plane near Army training point

Shear Zone:

Shearing is often found along few prominent joints or discontinuities. In the project site a small/narrow shear zone is found near the Sonamarg toll barrier. Huge amount of debris is formed covering this zone at a number of places. This zone is developed between hard compact volcanic Panjal traps and slatey natured fragile Zoji-La formation.This share zone runs along the contact between Panjal Trap and zoji-la formation in the direction N69^0 due N243^0 (Fig 37).

Fig 37 A View of Shear Zone near toll barrier Sonamarg

Ground Water Conditions

Area in the vicinity of tunnel alignment is rocky. Rocks are slightly porous due to vesicular structure whereas permeability is insignificant. Fluids flow through open joints and foliation planes only. Lithological characters of these rocks show that reservoir conditions do not exist at the site; still a spring is found flowing through a shear joint in the area at lower levels (Fig. 38). Source of water for this spring seems to be a distant one which is connected through joint planes.

Fig. 38 A View of Spring flowing through joints in the area.

Fig 39 A View of proposed Eastern Portal of Z-Morh Tunnel

Fig.40 A View of proposed Western Portal of Z-Morh Tunnel

Fig. 41 A view of High cliffs along the tunnel alignment

Fig.42 A View of high cliffs and Escarpment along tunnel alignment

Fig.43 A View of high cliff and steep Escarpments near Eastern portal

Fig.44 A View of steep escarpment from the top of western portal

TUNNEL ALIGNMENT

East-West trending alignment of tunnel stats from the village Gagangir, and goes upto village sitkhari. East portal is located on the right side of nala joining the river Sind near the Toll barrier of Sonamarg town (Fig 39), whereas Western portal falls on the left side of Sutiyan nala (Fig 40). In its alignment high cliffs, escarpments and steep slopes are encountered (fig 41 to 44). All along the tunnel alignment very high crest will be observed.

ENGINEERING GEOLOGY

Geotechnical properties of the rocks likely to be encountered at the site are being enumerated here.

Intact Rock Properties

The rock type mainly encountered at the site is metabasics followed by zozila formation in a small portion along the eastern portal. The summary of the intact rock properties is presented in Table 02. Due to various constrains at the site 38 mm diameter cores were used for testing. The chunks were drilled to get cores of 38 mm diameter. A lapping and polishing machine was used for grinding the end-surfaces of specimens to make end-surfaces parallel to each other and perpendicular to the axis of the core. Finally, end-surfaces were made smooth with polishing machine and manual grinding on fine sand.

Unit weight was obtained by calculating the volume of the cores and measuring their weights in air-dried conditions. For specific gravity, the rock was ground to powder form and density bottle was used to determine the specific gravity as per the procedure laid in IS2720-Part III, sec-2.

Brazilian tests were conducted on discoidal specimens in dry condition as per the procedure given in ISRM (1979) and IS:10082-1981. The load was applied continuously at a constant rate so that failure of rock occurred within 15 to 30 seconds. The tensile strength is calculated using the expression,

$$\sigma_t = \frac{2P}{\pi d.t} \qquad (4.1)$$

where,

P = load applied at failure; d=diameter of the specimen and

t = thickness of specimen.

Point load strength index test is an indirect test to get the uniaxial compressive strength and tensile strength of intact isotropic rock. The specimen is tested between two hardened conical tips having 5mm curvature and 60° conical angle in rigid frame. The point load strength index (I_{s50}) is given as:

$$I_{s50} = \frac{P}{d^2} \qquad (4.2)$$

Where P is the failure load and d is the size of the specimen (50 mm) measured after placing between the conical caps. The compressive strength is given by

$$\sigma_c = K\, I_{s50} \quad (4.3)$$

The value of K varies between 15 to 35 for most rocks; often it is taken in the range of 20-25 (Ramamurthy, 2007). In present case it is taken equal to 20. The tensile strength is given as (Ramamurthy, 2007)

$$\sigma_t = 1.25\, I_{s50} \quad (4.4)$$

When 50 mm size pieces are not available, the index is calculated by making size correction as follows:

$$I_{s50} = \left(\frac{d}{50}\right)^{0.45}\left(\frac{P}{d^2}\right) \quad (4.5)$$

Uniaxial compression tests were conducted on cylindrical specimens (l/d≈2.0) as suggested in ISRM (1979) suggested Methods and IS:9143-1979. Cylindrical cores of 38 mm diameter were used in the tests. Axial deformation was measured during the test. The tests were performed using a 3.0 MN conventional universal testing machine having an accuracy of ±0.1 kN. Teflon sheets of 0.5 mm thickness were introduced at the two ends of the specimens to facilitate uniform distribution of stresses and to minimize the end-friction. In each experiment, the axial loading was gradually increased with a uniform rate such that the failure occurred in 5-10 minutes. The failure of test specimens occurred due to vertical splitting in majority of cases. The values of tangent modulus E_{t50} was computed at 50% of failure stress. The Rocks were classified as per Deere and Miller classification (1966).

Conventional axi-symmetric triaxial compression tests were conducted on rock specimens of l/d≈2.0 as per ISRM (1981,1983) suggested methods and (IS:13047-1991). The shear strength parameters have been obtained using two failure criteria namely, Mohr-Coulomb and Hoek-Brown criterion. The Mohr-Coulomb parameters, c and ϕ have been obtained by plotting p-q diagram and fitting best straight line.

Mohr failure envelope: The original Hoek-Brown (1980) criterion was used to describe the non-linear strength behaviour of intact rocks. The confined strength of the intact rock is represented as follows:

$$\sigma_1 = \sigma_3 + \sqrt{m\sigma_{ci}\sigma_3 + \sigma_{ci}^2} \quad (4.6)$$

Where m and σ_{ci} are the criterion parameters,

σ_1 = the major principal stress at failure, σ_3 = the minor principal stress at failure.

The above equation was converted into linear form. The parameters were obtained by using least squares method.

Table 2. Summary of intact rock properties of Panjal Trap and Zoji-La formation

Property	Panjal Trap (Value)	Zoji-La Formation
Average unit weight	2.82 g/cc	2.45 g/cc
Specific gravity	2.9	2.3
Average tensile strength (Brazilian)	7.58 MPa	12.05MPa
Average UCS from point load index	177.92 MPa	85.88MPa
Average UCS from UCS tests	120.98 MPa	58.0MPa
Average E_{t50}	19.0 GPa	--
Deere-Miller classification	BL	--
Mohr-Coulomb shear strength parameters	c = 24.58 MPa, ϕ = 41.3°	--
Hoek-Brown strength parameters	σ_{ci}=108.15 MPa, m_i= 10.29	σ_{ci}=58.0 MPa m_i= 7.0

Rock Joint Properties

The geological observations discussed earlier present the details of the joints observed at the site. A rough idea about the joint properties can be obtained from these observations. It may however be noted that detailed mapping of joints along the tunnel alignment will be required to have higher confidence in the analysis. Nevertheless, for preliminary analysis these observations have been used. In general, there are four or more prominent joints sets encountered at various locations. A statistical analysis of dip-directions of the all the joints was carried out (Fig. 45). The analysis indicates the occurrence of the following three sets of joints plus random joints:

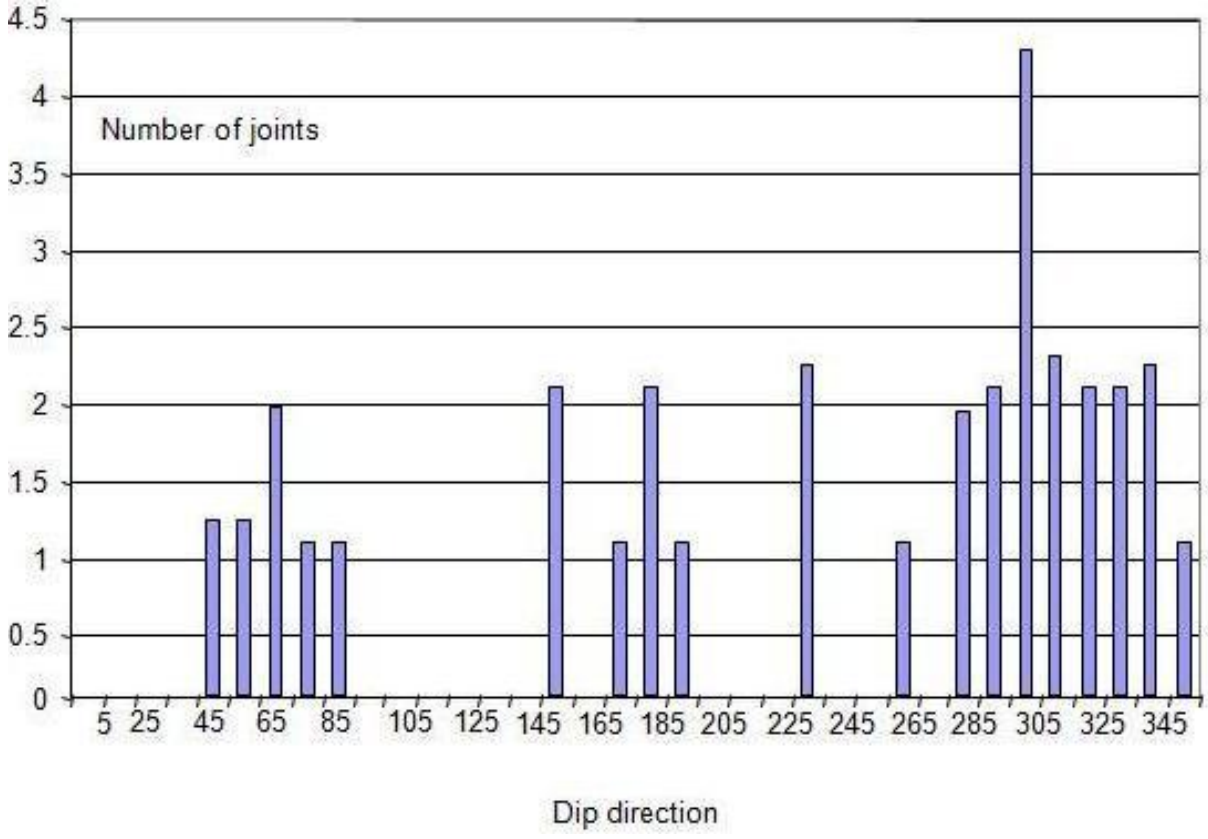

Fig. 45. Statistical analysis of dip-directions of joints (Z-Morh Tunnel Project)

Joint set I, Dip = 24°, dip-direction: 305°

Joiint set II Dip= 45°, dip-direction = 065°

Joint set III Dip = 70°, dip-direction= 185°.

The rocks in the area are reported to be foliated with average dip of 74° and dip-direction of 190°.

The assessment of the mechanical properties of the rock joints needs much more data from the exact location of the structures. The observations made on surface generally describe joints to be open. In the opinion of the authors, the joints will not remain open when acting under large overburden. It is therefore expected that the closed joints will be intersected in the tunnel accept close to the portals or if the overburden is low. At the site simple tests like tilt tests cab performed to get the frictional characteristics of the joint surfaces. In absence of such information Barton's model can be used to roughly estimate the shear strength parameters of rock joints. As per this model the shear strength along the joint is expressed as:

$$\tau_f = \sigma_n \tan\left[\phi_r + \text{JRC}\log_{10}\frac{\text{JCS}}{\sigma_n}\right] \quad (4.7)$$

where ϕ_r is residual friction angle, JRC is the joint roughness coefficient, which is a measure of the initial roughness (in degrees) of the discontinuity surface. JRC is assigned a value in the range of 0–20, by matching the field joint surface profile with the standard surface profiles on a laboratory scale of 10 cm (Barton and Choubey, 1977). JCS is the joint wall compressive strength of the discontinuity surface, and σ_n is the effective normal stress acting across the discontinuity surface.

In geological observations the discontinuities have been reported to be rough in majority cases. In very few cases smooth roughness is also reported. Simulated values of shear strength were plotted against normal stress; results are presented in Figs. 46. An approximate estimate of shear strength parameters is as follows:

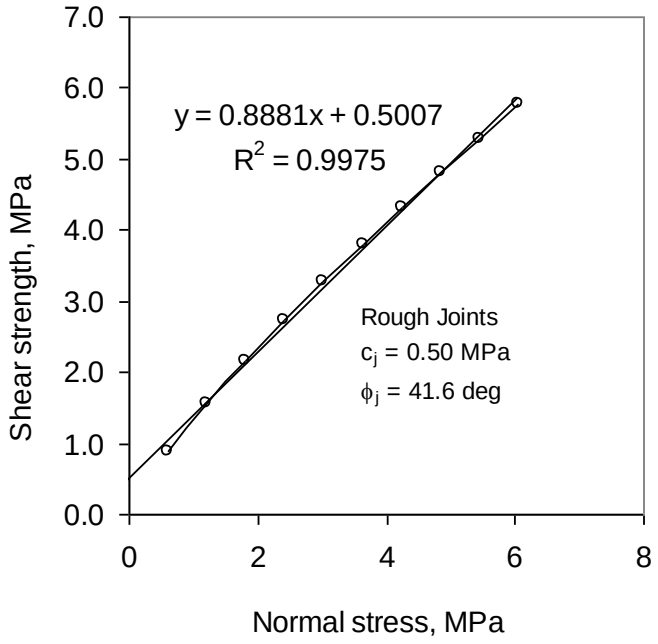

Fig 46.a. Simulated shear strength envelope from Barton's model

(Rough joints: JRC= 12)

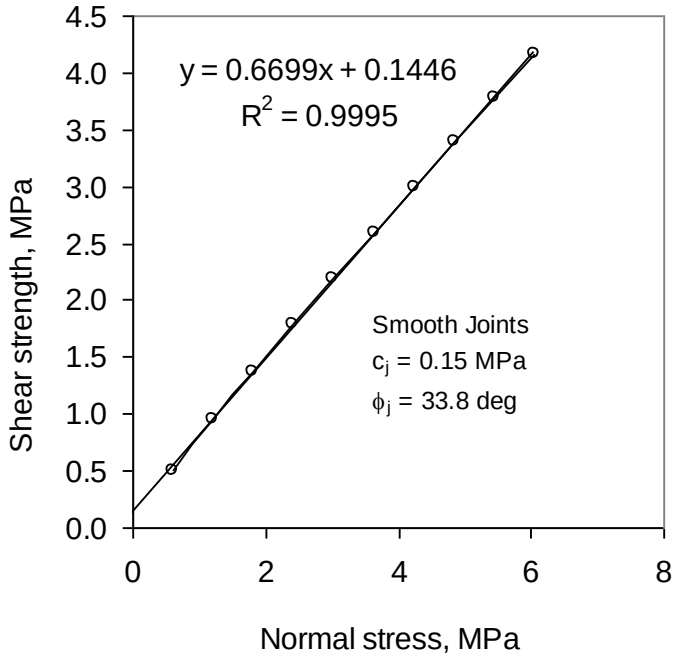

Fig 46.b. Simulated shear strength envelope from Barton's model

(Smooth joints: JRC= 5)

i. Rough joints; c_j = 0.50 MPa, ϕ_j = 41.6 degrees.

ii. Smooth joints c_j = 0.15 MPa, ϕ_j = 33.8 degrees.

Rock Mass Modulus

The best estimate of rock mass deformability can only be made from the results of the field tests. This data will be available only after the detailed investigation. In the absence of such data, deformability characteristics may be estimated approximately from classification approaches and laboratory test data.

Hoek and Diederichs (2006) have suggested the following expressions for the rock mass modulus based on GSI:

$$E_{mass} = E_i\left(0.02 + \frac{1-D/2}{1+\exp((60+15D-GSI)/11)}\right) \quad (4.8)$$

$$E_{mass} = 1x10^5\left(\frac{1-D/2}{1+\exp((75+25D-GSI)/11)}\right) \quad (4.9)$$

where E_i is the intact rock modulus and D is the damage factor.

Barton (2002) has suggested the following expression for rock mass modulus in terms of rock mass quality, Q:

$$E_{mass} = 10Q_c^{1/3} \text{ GPa} \quad (4.10)$$

$$\text{Where } Q_c = Q\frac{\sigma_{ci}}{100} \quad (4.11)$$

σ_{ci} is the intact rock strength in MPa.

The Rock Mass Rating (RMR) may be used to estimate rock mass modulus as follows:

- Serafim and Pereirra (1983)

$$E_{mass} = 10^{(RMR-10)/40} \text{ GPa} \quad (4.12)$$

- Mehrotra (1992):

$$E_{mass} = 10^{(RMR-25)/40} \text{ GPa} \quad (4.13)$$

- Ramamurthy (2007)

$$E_{mass} = E_i \exp\left(\frac{RMR - 100}{17.4}\right) \quad (4.14)$$

Geotechnical investigations are required to be done with an aim of characterising the rock mass available at different section along the tunnel alignment. It is suggested that various classification systems (RQD, Q, RMR and GSI) should be used independently to characterise the rock mass. The rock mass then should be divided into several classes and should be analysed for tunnel support pressure etc. In absence of any such detailed investigation a rough exercise was done by using the photographs of various locations. GSI was assigned and RMR and Q were estimated from assigned GSI. The following expressions were used to estimate Q and RMR.

$$GSI = RMR-5 \quad (4.15)$$

$$RMR = 9 \ln Q + 44 \quad (4.16)$$

The rock mass modulus values obtained from the above expressions are presented in Table 3. The average values of the estimated rock mass modulus are also presented in the table 3.

Table 3. Estimated rock mass modulus from different approaches

Sl	GSI	RMR	Q	Rock mass modulus (GPa)						
				Hoek and Diederichs (2006)-1	Hoek and Diederichs (2006)-2	Barton (2002)	Ramamurthy (2007)	Mehrotra (1992)	Serafim and Pereirra (1983)	Average
1	25	30	0.211	1.137	1.050	6.344	0.340	1.334	3.162	2.228
2	30	35	0.368	1.546	1.645	7.635	0.453	1.778	4.217	2.879
3	40	45	1.118	3.033	3.986	11.057	0.805	3.162	7.499	4.924
4	50	55	3.395	5.837	9.341	16.014	1.431	5.623	13.335	8.597
5	60	65	10.312	9.880	20.365	23.193	2.542	10.000	23.714	14.949

Uniaxial Compressive Strength of Rock Mass

Rock mass strength under uniaxial loading condition has been estimated by the following approaches:

i) Yudhbir & Prinzl (1983)

$$\frac{\sigma_{cm}}{\sigma_{ci}} = \exp\left(\frac{7.65 \text{ x } (RMR - 100)}{100}\right) \quad (4.17)$$

ii) Laubscher (1984) and Singh and Goel (1999)

$$\frac{\sigma_{cm}}{\sigma_{ci}} = \frac{RMR - \text{Rating for } \sigma_{ci}}{106} \quad (4.18)$$

iii) Ramamurthy et al. (1985) and Ramamurthy (1986)

$$\frac{\sigma_{cm}}{\sigma_{ci}} = \exp\left(\frac{RMR - 100}{18.75}\right) \quad (4.19)$$

iv) Trueman (1988) and Asef et al. (2000)

$$\sigma_{cm} = 0.5 \exp(0.06\ RMR) \text{ MPa} \quad (4.20)$$

v) Kalamaras and Bieniawski (1993)

$$\frac{\sigma_{cm}}{\sigma_{ci}} = \exp\left(\frac{RMR - 100}{24}\right) \quad (4.21)$$

vi) Sheorey (1997)

$$\frac{\sigma_{cm}}{\sigma_{ci}} = \exp\left(\frac{RMR - 100}{20}\right) \quad (4.22)$$

vii) Aydan and Dalgic¸ (1998)

$$\frac{\sigma_{cm}}{\sigma_{ci}} = \frac{RMR}{RMR + 6(100 - RMR)} \quad (4.23)$$

viii) Singh and Rao (2005)

$$\frac{\sigma_{cm}}{\sigma_{ci}} = \left(\frac{E_{mass}}{E_i}\right)^{0.63} \quad (4.24)$$

where σ_{cm} = rock mass strength

E_{mass} = rock mass modulus

E_i = intact rock modulus.

ix) Singh et al. (1997)

$$\sigma_{cm} = 7\gamma Q^{1/3} \quad \text{(for } Q<10,\ 2<\sigma_{ci}<100 \text{ MPa, SRF = 2.5)} \qquad (4.25)$$

where γ is unit weight in gm/cc.

x) Barton (2002)

$$\sigma_{cm} = 5\gamma\left(\frac{Q\sigma_{ci}}{100}\right)^{1/3} \qquad (4.26)$$

The above mentioned approaches were used to estimate the rock mass strength values. The results are presented in Table 4 where average values are also reported. It can be noted that depending on characterisation of a particular location the average value of rock mass strength may be taken in the range of about 14 to 51 MPa.

Table 4. Estimated rock mass strength

Sl	GSI	RMR	Q	Rock mass strength (MPa)														
				Yudhbir & Prinzl, MPa	Laubscher (1984)	Ramamurthy (1993)	Trueman (1988)	Kalamaras & Bieniawski (1993)	Sheorey (1997)	Aydan & Dalgic (1998)	E_{mass} from Deiderich -1	E_{mass} from Hoek, Deiderich -2	E_{mass} from Barton	E_{mass} from Ramamurthy (RMR)	E_{mass} from Mehrotra (1992)	Barton (2002)	Singh et al, (1997)	Average
1	25	30	0.211	0.57	20.54	2.89	3.02	6.55	3.65	8.07	20.53	19.52	60.62	9.59	22.69	7.93	10.42	14.04
2	30	35	0.368	0.84	26.25	3.78	4.08	8.06	4.69	9.96	24.91	25.90	68.12	11.50	27.20	9.54	12.54	16.96
3	40	45	1.118	1.80	37.66	6.44	7.44	12.23	7.73	14.52	38.08	45.23	86.02	16.51	39.09	13.82	18.16	24.62
4	50	55	3.395	3.87	49.08	10.98	13.56	18.55	12.75	20.47	57.51	77.35	108.63	23.72	56.18	20.02	26.30	35.64
5	60	65	10.312	8.32	60.49	18.71	24.70	28.14	21.02	28.60	80.13	126.39	137.17	34.07	80.74	28.99	38.09	51.11

Triaxial Strength of Rock Mass

Mohr-Coulomb shear strength parameters of the rock mass (c_{mass} and ϕ_{mass}) are required to compute the triaxial strength of the rock mass. A procedure suggested by Hoek and Brown (1997) has been adopted for this purpose. As per this approach, the strength of the rock mass is represented by the generalised criterion as:

$$\sigma_1 = \sigma_3 + \sigma_{ci}\left(\frac{m_j\sigma_3}{\sigma_{ci}} + s_j\right)^a \qquad (4.27)$$

The parameters, m_j, s_j and 'a' are estimated from the following relationships:

$$m_j = m_i e^{\left(\frac{GSI-100}{28}\right)} \qquad (4.28)$$

i) For undisturbed rock masses i.e GSI > 25

$$s_j = e^{\left(\frac{GSI-100}{9}\right)} \qquad (4.29)$$

$$a = 0.5$$

ii) For disturbed rock masses, GSI < 25

$$s = 0$$

$$a = 0.65 - \frac{GSI}{200} \qquad (4.28)$$

where, GSI is the geological strength index.

By following the above expressions, parameters m_j, s_j and 'a' were obtained for two extreme GSI values i.e. 22 and 62 respectively. Now the values of simulated tri-axial strength were generated for eight confining stresses in the range of $0<\sigma_3<0.25\ \sigma_{ci}$ as suggested by Hoek and Brown (1997). The equivalent Mohr-Coulomb shear strength parameters, c_{mass} and ϕ_{mass} were now obtained by fitting a straight line into the simulated tri-axial tests data and using the following expressions:

$$\phi_{mass} = \sin^{-1}\left(\frac{k-1}{k+1}\right) \qquad (4.29)$$

$$c_{mass} = \frac{\sigma_{cm}}{2\sqrt{k}} \quad (4.30)$$

where the best fitting straight lie is given as:

$$\sigma_1 = \sigma_{cm} + k\sigma_3 \quad (4.31)$$

The results are presented in Figs. 47**.** The representative values of the shear strength parameters of the rock mass are presented in Table 5.

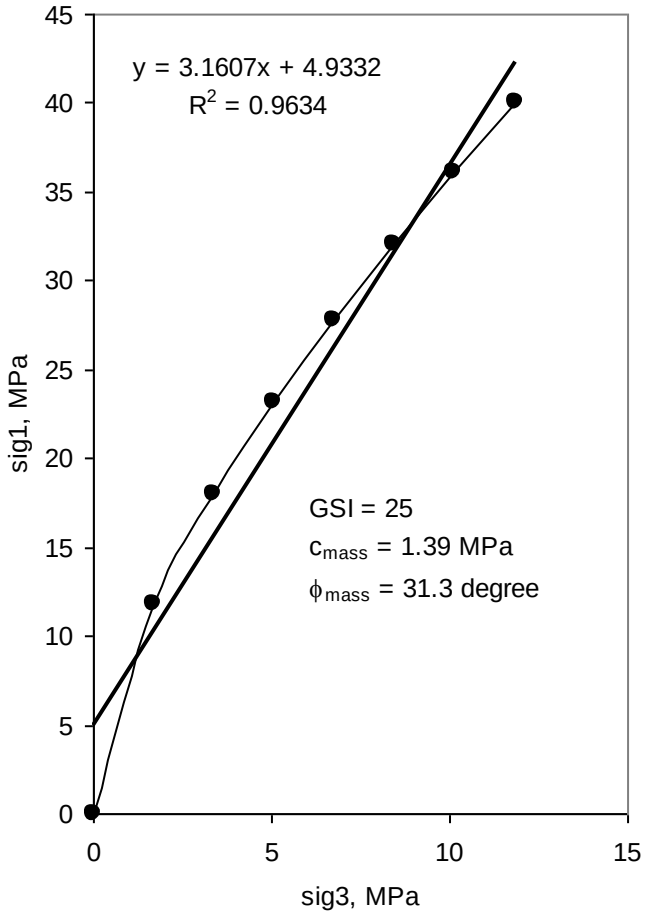

Fig. 47 a. Shear strength parameters of rock mass through Hoek-Brown failure (GSI = 35)

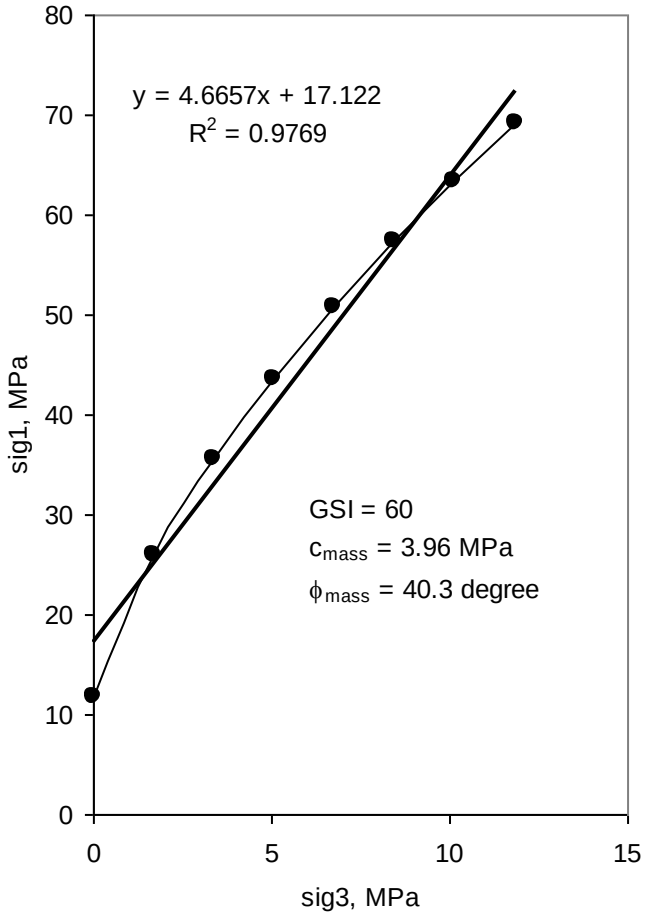

Fig. 47 b. Shear strength parameters of rock mass through Hoek-Brown failure (GSI = 60)

Table 5. Hoek- Brown and equivalent Mohr-Coulomb shear strength parameters

GSI	m_i	σ_{ci}, MPa	m_j	s_j	a	c_{mass} MPa	ϕ_{mass} (degrees)
25	10.29	108.15	1.0098	0.00073	0.50	2.15	34.3
60	10.29	108.15	2.47	0.0117	0.50	3.96	40.3

Squeezing and rock burst

If the rock cover above tunnel roof exceeds about 900 m rock bursting or squeezing conditions may be expected. The degree of squeezing may be obtained from the ratio of circumferential stress to the strength of the rock mass at the periphery of the tunnel as given in Table 6. In the present case rock mass strength has been found to vary between 14to 51 MPa depending on the rock mass characterization. Taking maximum circumferential stress equal to 2 γH, the σ_θ for overburden of 900 works out to be 45 MPa. The ratio σ_θ/ σ_{cm} may vary from 3.21 to 0.88. This indicates that conditions from moderate squeezing/ bursting to no squeezing may be encountered during tunnel construction. The intermediate principal stress may however play important role and squeezing may reduce due strength enhancement due to intermediate principal stress.

Table 6 Suggested predictions of squeezing conditions

Degree of squeezing	σ_θ/ σ_{cm} (ISRM)	σ_{cm} /(γH) (Barla)
Non squeezing	< 1.0	>1.0
Mild squeezing	1.0 – 2.0	0.4 – 1.0
Moderate squeezing	2.0 – 4.0	0.2 – 0.4
High squeezing	> 4.0	<0.2

BIBLIOGRAPHY

Auden, J.B., 1935, Traverses in the Himalayas, Rec. Geol. Surv. Ind., 69 (2) Bologne.

Asef M. R., Reddish D. J., Lloyd P. W. (2000) Rock-support interaction analysis based on numerical modeling, *Geotech. Geol. Eng.,* 18:23–37.

Aydan O., Dalgic S. (1998) Prediction of deformation behavior of 3-lanes Bolu tunnels through squeezing rocks of North Anatolian fault zone (NAFZ). In: *Proceedings of regional symposium on sedimentary rock engineering*, Taipei, pp 228–233.

Barla, G., 2001. Tunnelling under squeezing rock conditions. Tunnelling mechanics. In: *Kolymbas* (Ed.), Eurosummer-School in Tunnel Mechanics, Innsbruck, 2001, Logos Verlag, Berlin, pp. 169–268. Available at: http://ulisse.polito.it/matdid/ 1ing_civ_D3342_TO_0/ Innsbruck2001.PDF>.

Barton N. (2002) Some new Q-value correlations to assist in site characterisation and tunnel design, *Int. Jl. Rock Mech. & Min. Sci.,* 39: 185–216.

Barton, N. and Chobey, V. (1977), "The Shear Strength of Rock Joints in Theory and Practice", Rock Mechanics, 10, 1-54.

Desio, A., Tongiorgi, E. and Ferrara, G., 1964, on the geological age of some granites of Karakoram, Hindukush and Badakhshan (Central Asia), Proc, 22nd. Inter. Geol. Cong., 2, 479-496.

Hoek E. and Bray J.W. (1981) *Rock Slope Engineering*, Revised 3rd edition, The Institution of Mining and Metallurgy, London, pp 341 – 351.

Hoek E., Brown E.T. (1997) Practical estimates of rock mass strength. *Int. Jl. Rock Mech. Min. Sci.,* 34:1165–1186.

Hoek E., Diederichs M. S. (2006) Empirical estimation of rock mass modulus. *Int. Jl Rock Mech. Min. Sci.,* 36:203–215.

Kalamaras G. S., Bieniawski Z. T. (1993) A rock mass strength concept for coal seams. In: Proceedings of *12th conference ground control in mining*, Morgantown, pp 274–283.

Laubscher D. H., (1984) Design aspects and effectiveness of support system in different mining conditions. *Trans. Inst. Min. Met.*, 93:A70–A81.

Mathur, Y, K. and Jain, A. K ., 1973, palynology and age of the Dras Volcanics near Shergol,

Mehrotra V. K. (1992) *Estimation of Engineering Parameters of Rock Mass*, Ph.D. thesis, University of Roorkee, Roorkee, India.

Ramamurthy T., Rao G.V., Rao K. S. (1985) A strength criterion for rocks. In: *Proceedings of Indian geotechnical conference*, Vol 1, Roorkee, pp 59–64.

S.K Shah, Madan L. Sharma, J. T. Gergan and C.S. Tara (1976), Stratigraphy & Structure of the Western part of the Indus Suture Belt, Ladakh, Northwest Himalaya., Deptt. Of Geology, University of Jammu, Jammu.

Serafim J. L., Pereira J. P. (1983) Consideration of the geomechanical classification of Bieniawski. In: *Proceedings of international symposium on engineering geology and underground construction*, Lisbon, Portugal, Vol 1(II), pp 33–44.

Sheorey P. R. (1997) *Empirical rock failure criteria*. Balkema, Rotterdam.

Singh B, Viladkar MN, Samadhiya NK, Mehrotra VK. (1997) Rock mass strength parameters mobilised in tunnels. Tunnelling and Underground Space Technology, 12(1), 47 - 54.

Singh M., Rao K. S. (2005) Empirical methods to estimate the strength of jointed rock masses. *Eng. Geol.,* 77(1–2):127–137.

Trueman R. (1988) An evaluation of strata support techniques in dual life gateroads. Ph.D. thesis, University of Wales, Cardiff.

Yudhbir W. L., Prinzl F. (1983) An empirical failure criterion for rock masses. In: *Proceedings of 5th international congress on Rock Mechanics*, Vol. 1, Melbourne, pp B1–B8.

Wadia ,D.N., 1937, The cretaceous and Volcanic series of Astor, Deosai Kashmir and its Intrusions, Rec. Geol. Surv. India. 72 (2), 151-61.